IEEE Access
Multidisciplinary ⋮ Rapid Review ⋮ Open Access Journal

Received 11 September 2022, accepted 21 September 2022, date of publication 26 September 2022,
date of current version 7 October 2022.

Digital Object Identifier 10.1109/ACCESS.2022.3210165

RESEARCH ARTICLE

Multiobjective Optimization of Roadheader Shovel-Plate Parameters Using Gray Weight and Particle Swarm Optimization

QIANG LI[1,2], SONGYONG LIU[1], AND MENGDI GAO[2]
[1]School of Mechatronic Engineering, China University of Mining and Technology, Xuzhou 221116, China
[2]School of Mechanical and Electronic Engineering, Suzhou University, Suzhou 234000, China

Corresponding author: Songyong Liu (liusongyong@163.com)

This work was supported in part by the Scientific Research Project of Anhui Universities under Grant KJ2021A1106, in part by the Natural Science Foundation of Anhui Province under Grant 2008085QE265, in part by the Suzhou Science and Technology Project under Grant 2019019, and in part by the Scientific Research Platform Open Project of Suzhou University under Grant 2020ykf12.

ABSTRACT As the working efficiency and life span of the shovel plate of a roadheader directly influence its performance, optimization of the shovel-plate parameters is crucial. For optimizing the shovel-plate parameters, the variations in the loading capacity and shovel grubbing force with respect to the shovel-plate parameters are determined in this study. Moreover, the ideal point method and gray weight method are proposed for multiobjective optimization. The gray weights of the loading capacity and shovel resistance are determined by investigating existing molded products and through the gray decision method. Thereafter, the particle swarm optimization (PSO) algorithm is applied for multiobjective optimization of the shovel-plate parameters. Considering the EBZ230-type roadheader shovel plate as an example, parameter optimization through multiobjective optimization decreases the mass of the shovel plate by 14.3% and the shovel resistance by 7.3%, while increasing the loading capacity by 1.4%. To demonstrate the influence of optimization, coal and rock excavation with a shovel is simulated using the optimized parameters in an ANSYS-Workbench environment. The results indicate that the maximum stress at the front of the shovel plate decreases by 22.1%, minimum fatigue life increases by 139.6%, and minimum safety factor increases by 30.3%. The obtained results establish that, in multiobjective optimization based on PSO, the ideal point method and gray weight method optimize the shovel-plate parameters. This optimization can provide a theoretical basis and reference values for the design of roadheader shovel plates and can be applied for multiobjective optimization in engineering as well.

INDEX TERMS Multiobjective optimization, particle swarm algorithm, roadheader, shovel plate.

I. INTRODUCTION

According to the BP World Energy Statistical Yearbook and BP World Energy Outlook 2021, over the following 20 years, coal is expected to account for more than 25% of the global primary energy consumption, with oil comprising the major proportion [1]. Thus, coal will remain the primary energy source in the foreseeable future [2]. China is currently the largest coal producer and consumer. Due to energy structure restrictions and the demand for rapid development of the national economy, the demand for coal is expected to increase continuously. Although the coal mining and transportation efficiencies are superior in China, the coal tunneling efficiency is subject to a bottleneck that restricts the improvement of coal outputs [3]. Cantilever roadheaders are generally used for coal roadway excavations [4]. In July 2020, the high-quality development guidance draft of the 14th five-year plan by the China coal industry indicated that the degree of coal mining and excavation mechanization was 90% and more than 75%, respectively [5]. In December 2021, guidelines for

The associate editor coordinating the review of this manuscript and approving it for publication was Kuo-Ching Ying.

safe and efficient coal mine construction in the 14th five-year plan of the coal industry were issued, and it was noted that advanced and applicable technologies and equipment should be popularized. Moreover, it was suggested that automation and intelligent construction should be promoted for the safe deepening of small- and medium-sized coal mines and for enhancing the efficiency of coal mines through mechanized replacement and automated specialized tasks. By 2025, the mechanization of coal mining and tunneling is expected to reach 99% and an average of 90%, respectively [6].

The development of intelligent core technologies and equipment is expected to increase. Moreover, the development of intelligent mining technology and equipment suitable for different conditions is anticipated, focusing on breakthroughs in applications such as intelligent, fully-mechanized mining and rapid tunneling under complex conditions [7]. This indicates an improvement in the speed and quality of roadway excavation; therefore, optimizing the performance and improving the operational stability of the roadheader is critical [8]. Wang established a dynamic model for the transmission system of the cutting unit and analyzed the torsional vibration characteristics of existing roadheaders [9]. Zhang analyzed the vibration of the roadheader rotary table based on the finite element method and data from an underground coal mine, where the control parameters could be adjusted in real time [10]. Furthermore, the dynamic model and control method were simulated in MATLAB, and the control method was tested using a roadheader control experiment system [11]; the designed control system satisfied the control requirements. Shen proposed an error compensation method based on the vibration characteristics of the roadheader to further analyze the angular and linear vibration of the fuselage [12]. Experimental results revealed that the proposed error compensation algorithm could eliminate the influence of angular and linear vibration on the measurement accuracy. Ji established kinematic and dynamic models for the roadheader path rectification at low speeds and under complex working conditions. The obstacle-crossing ability of roadheaders was calculated in the course of path rectification in modes based on the roadway conditions, in addition to the crawler resistance and driving performance of the roadheader [13]. Liu highlighted the importance of improving the ecoefficiency and production efficiency, which is coincident with enterprise requirements [14]. Fang proposed principal component analysis (PCA) and multiobjective particle swarm optimization (MPSO) algorithms to improve the analysis speed and accuracy of posture deviation; a parallel dynamic co-operative optimization (PDCO) strategy was incorporated to accurately adjust posture deviations [15]. Liu proposed the use of an improved particle swarm optimization (PSO) algorithm to efficiently optimize the remanufacturing value of waste parts [16].

Although improvements in roadheader performance, such as those in the cutting stability and walking reliability, have been researched extensively, studies on roadheader shovel plates remain limited. The shovel plate is one of the main working parts of the roadheader, and its working efficiency and life span directly influence the roadheader performance. Therefore, optimization of the shovel-plate parameters is critical for improving the overall performance of the roadheader [17]. Shovel plate parameters optimization are multi - objective optimization problems. Many scholars have used intelligent algorithms to deal with multi - objective optimization problems and have achieved great results. Ulu builded orientation optimization algorithm, and demonstrated their method on a variety of 3D models and validate it by 3D printing [18]. Moore and Venayagamoorthy proposed a quantum PSO for combinational logic circuits [19]. Mikki and Kishk21 proposed a quantum PSO algorithm for optimizing electromagnetism problems [20]. Zhang proposed a PSO algorithm based on the mixture of priority and simulated annealing sampling to handle the problem of hybrid assembly lines [21]. Wei improved PSO based on a globally optimal leading-particle-selection strategy with individual disturbance for rolling schedule optimization of a five-stand tandem cold mill [22].

In view of the above, this study performs multiobjective optimization of the shovel-plate parameters for the optimal design to improve the load capacity and reduce the propulsive resistance of the shovel. The ideal point method and gray weight are incorporated in the multiobjective optimization [23], [24]. As the PSO has a high-convergence speed, is simple to implement, and involves only a few parameters that require adjustment [25]. Therefore, based on the PSO algorithm, the ideal point method and gray weight multiobjective processing method are adopted to determine the optimal shovel-plate parameters. Furthermore, the results before and after optimization are compared and analyzed.

In this study, based on the particle swarm optimization algorithm, the multi-objective processing method combining ideal point method and gray weight is used to optimize the shovel plate parameters, and the results before and after optimization are compared and analyzed. Major contributions of the study are outlined as follows:

1) This study developed a method combining the ideal point method and gray weight method for constructing an objective function for multiobjective optimization. In addition, a method for objectively determining the index weight coefficient is provided. It can avoid the organization and coordination of field experts and professionals to determine the weight and can also overcome the ideal point method can not reflect each the importance of the target function.

2) The above method is used to carry out multi-objective optimization of shovel plate parameters. The optimization results are obtained using PSO, and the results before and after optimization are compared and analyzed.

The remainder of this paper is organized as follows: Section II introduces the formulation method combining the ideal point and gray weight for multiobjective optimization. In Section III, the application of the method for multiobjective optimization of roadheader shovel-plate parameters is

demonstrated. In Section IV, simulation analysis and comparative analysis before and after optimization are presented.

II. MATERIALS AND METHODS

A. METHOD FLOW

Multiobjective optimization is a critical process in scientific research and engineering applications [26]. Most practical engineering optimization problems are multiobjective ones. Each objective function of a multiobjective optimization problem is maximized or minimized. The dimensions and significance of each objective function are entirely different, resulting in complexity. Hence, it is necessary to unify the goals of the objective functions, i.e., convert functions that require maximization to those that require minimization: $\max f_i(X) = -\min(f_i(X))$. Similarly, the inequality constraint $g_i \geq 0 (i = 1, 2, \ldots, k)$ can be converted to $g_i(X) \leq 0 (i = 1, 2, \ldots, k)$. Thus, any form of multiobjective optimization problem can be transformed into a unified expression as follows [27]:

$$\begin{cases} \min f(X) = (f_1(X), & f_2(X), \ldots, f_r(X)) \\ s.t.\ \ g_i(X) \leq 0, & (i = 1, 2, \ldots k) \\ h_j(X) = 0, & (j = k+1, \ldots, m) \\ x_i^{\min} \leq x_i \leq x_i^{\max}, & (i = 1, 2, \ldots, n) \end{cases} \tag{1}$$

Optimization involves determining $X^* = (x_1^*, x_2^*, \ldots, x_n^*)$ such that $f(X^*)$ is optimal for a set of constraints. However, in general, X^* such that the objective functions are optimal for all r do not exist. Therefore, different methods should be adopted to handle multiobjective problems based on their characteristics. Several methods are available for overcoming this problem, such as transformation into single-objective problems, which is common practice [28], [29], [30].The most common way to deal with multiobjective optimization problems is to transform them into single objectives [31], [32], [33].

The underlying principle of the ideal point method is to determine a point situated maximally close to the ideal point under the guidance of modules. In general, the objective function is constructed using the modulo distance in Euclidean space $z = \min\left(\sum_{i=1}^{r}(f_i - f_i^*)^2\right)$, where f_i^* is the ideal value of each objective function under the constraint conditions.

The core idea of the linear weighting method is the assignment of a non-negative weight coefficient according to the importance of each objective function, $w_i \geq 0 (i = 1, 2, \ldots, r)$, $\sum_{i=1}^{r} w_i$. These weighted objectives are then added to construct an evaluation function $z = \min(\sum_{i=1}^{r} w_i f_i(x))$.

Each objective function has a different physical meaning and dimensionality in engineering practice, and the degree of consideration is not uniform [34], [35]. The ideal point method cannot be used to distinguish the importance of each objective function [36], [37]. However, the simple linear weighting method is excessively subjective, and it is difficult and expensive to organize and coordinate experts and professionals in the field to ascertain the weights [38], [39].

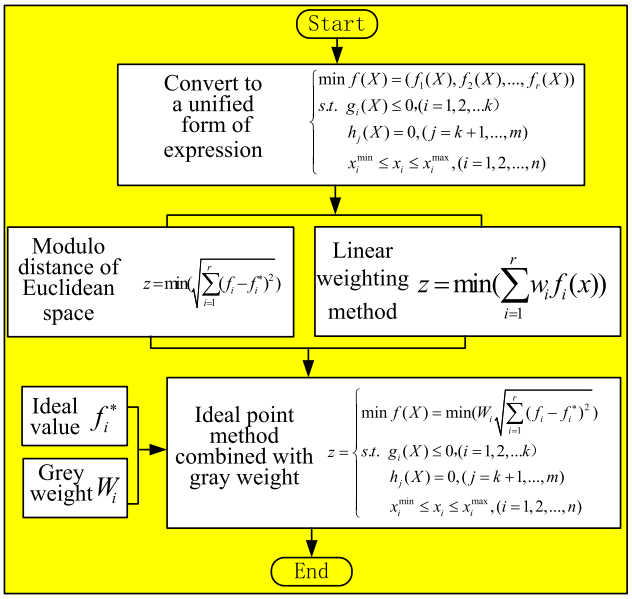

FIGURE 1. Flowchart of proposed method.

In this study, an attempt was made to construct an objective function for multiobjective optimization by combining the ideal point method and gray weight (the weight of each index is calculated using the gray relational degree theory) to overcome the abovementioned shortcomings.

The multiobjective optimization processing function constructed based on the ideal point method and gray weight can be expressed as follows:

$$\begin{cases} \min f(X) = \min(W_i \sqrt{\sum_{i=1}^{r}(f_i - f_i^*)^2}) \\ s.t.\ \ g_i(X) \leq 0, & (i = 1, 2, \ldots k) \\ h_j(X) = 0, & (j = k+1, \ldots, m) \\ x_i^{\min} \leq x_i \leq x_i^{\max}, & (i = 1, 2, \ldots, n) \end{cases} \tag{2}$$

The flowchart for multiobjective optimization based on the PSO combining the ideal point method and gray weight is depicted in Fig. 1. The pseudocode [40] for the proposed PSO combining the ideal point method and gray weight is detailed in Algorithm 1.

Computational complexity is an important indicator to measure algorithm efficiency [41], [42]. The complexity of the proposed method combining the ideal point method and gray weight PSO is as follows.

1) TIME COMPLEXITY

The initialization particle of the proposed ideal point method and gray weight PSO has of complexity of $O(N \times Dim)$, where N represents the particle size and Dim represents the variable dimension. The calculated fitness value of the particle takes $O(N \times f \times S)$ time, where f is the objective function that defines the problem, and S represents the maximum

Algorithm 1 The PSO Combining the Ideal Point Method and Gray Weight

Input: The population size N; accelerated factor c_1, c_2; iterative algebra S;
Output: The best particle *zbest* and its fitness value *fitnesszbest*; the best group *gbest* and its fitness value *fitnessgbest*
1: Initialize the population randomly
2: Combining the ideal point method and gray weight deal with the individual target functions using Eq. (2)
3: Calculate the fitness value f of each particle *fitnesszbest*
4: Determine the particle optimum position *zbest* and the swarm optimum position *gbest*
5: Update each particle using Eq. (10)
6: The particles generated in each iteration are checked by constraint popmax and popmin (for ii= 1:sizepop;for jj=1:size(pop,2);if pop(ii,jj)<popmin(jj);pop(ii,jj)=popmin(jj);end)
7: The new particles are produced again for inspection(pop(j,:)=pop(j,:)+V(j,:));
8: Recalculated the fitness value of each particle *fitnesszbest*
9: Compare the fitness value of each particle(if fitness_Q(j) > *fitnessgbest*(j); *gbest*(j,:) = pop(j,:); *fitnessgbest*(j) = fitness_Q(j); end)
10: Update group optimal location(if fitness_Q(j) > *fitnesszbest*; *zbest* =pop(j,:); *fitnesszbest*= fitness_Q(j);end)
11: **End if**
12: End while
13: Return *gbest* and *fitnessgbest*

number of iterations. In each iteration, it takes $O(M)$ time to find the current optimal solution. The total time complexity of the ideal point method and gray weight PSO in the iteration stage is $O(M \times S \times N \times f \times Dim)$.

2) SPACE COMPLEXITY [43]

Initializing the particle can be regarded as the maximum amount of space occupied by the ideal point method and gray weight PSO at any time. Therefore, the space complexity of the proposed algorithm is $O(N \times Dim)$.

B. GRAY WEIGHTS

Based on the gray relational degree theory, a method for objectively determining the index weight coefficient is provided using the gray relational degree of the factor index, as follows:

1) Obtain the initial data based on research and with reference to relevant literature.

2) Select the most critical factors influencing the scheme as the mother index and denote the index value corresponding to the parent index as $X_0 = (x_{10}, x_{20}, \ldots x_{n0})^T$ and a parent sequence. Select the other factors as subindices. Thereafter, the index value corresponding to the subindex is denoted as $X_j = (x_{1j}, x_{2j}, \ldots x_{nj})^T (j = 1, 2, \ldots, m)$ and a subsequence.

3) Initialize X_0 and X_j and denote

$$x'_{i0} = x_{i0}/x_{10}, x'_{ij} = x_{ij}/x_{1j}$$
$$X'_0 = (x'_{10}, x'_{20}, \ldots x'_{n0})^T \quad (3)$$

and $X'_j = (x'_{1j}, x'_{2j}, \ldots x'_{nj})^T$. The initialization index value matrix is obtained as $\mathbf{A} = (X'_0, X'_j)$.

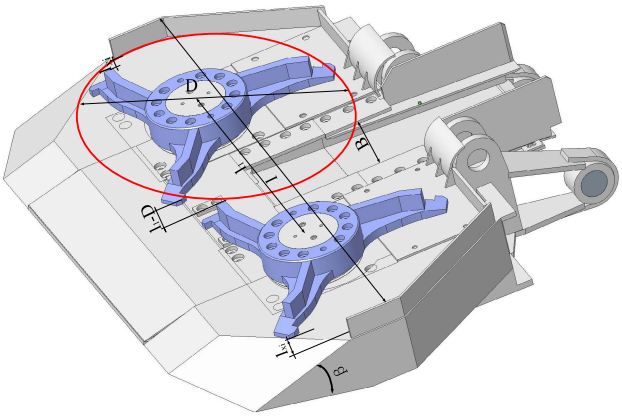

FIGURE 2. Schematic of shovel plate parameters.

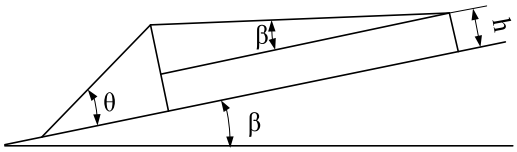

FIGURE 3. Accumulation of coal and rock on shovel surface.

4) Thereafter, calculate the correlation coefficients $\boldsymbol{r}_{ij}$ of X_j and X_0 to construct correlation coefficient matrix $\mathrm{R} = (r_{ij})_{n\times m}$.

$$r_{ij} = \frac{\min\limits_{1\le i\le n_1}\min\limits_{1\le j\le m}\left|x'_{ij} - x'_{oj}\right| + \rho \max\limits_{1\le i\le n_1}\max\limits_{1\le j\le m}\left|x'_{ij} - x'_{oj}\right|}{\left|x'_{ij} - x'_{oj}\right| + \rho \max\limits_{1\le i\le n_1}\max\limits_{1\le j\le m}\left|x'_{ij} - x'_{oj}\right|}, \quad (4)$$

where $\rho(0 < \rho < 1)$ is the resolution coefficient, which is generally set as 0.5, reducing the distortion and improving the difference between the correlation coefficients.

5) Average the columns of matrix R as $r_j = \frac{1}{n}\sum_{i=1}^{n} r_{ij}$ and r_j as follows:

$$W_j = r_j / \sum_{j=1}^{m} r_j, j = 1, 2, \ldots, m. \quad (5)$$

Gray weights $W_1, W_2, \ldots W_m$ are obtained for the indicators.

C. ESTABLISHMENT OF OPTIMAL MODEL FOR SHOVEL PLATE

1) RELATIONSHIP BETWEEN LOADING CAPACITY AND SHOVEL-PLATE PARAMETERS

Considering the amount of material that can enter the chute of the first transport plane, the accumulation of coal rock, the shovel-plate schematic (Fig.2), and the accumulation of coal rock on the shovel-plate surface (Fig.3).

The accumulation of coal rock on the shovel surface can be determined as follows:

$$Q = \frac{\pi D \eta_m n}{2}(B + 2D + 2l_{xi} - l)(2h + \frac{D}{4}\tan\beta)K_z, \quad (6)$$

where Q is the load capacity in cubic meters per minute (m^3/min), D is the outer-diameter of the star wheel in meters (m), n is the star wheel speed in revolutions per minute (r/min), B is the conveyor trough width in meters (m), l_{x_i} is the gap between the outer-edge of the wheel claw and the shovel plate in meters (m), l is the width of the shovel plate in meters (m), H is the height of the wheel claw in meters (m), β is the inclination angle of the shovel plate in degrees (°), $K_Z = 0.25 \sim 1$ is the loading coefficient, and η_m is the motor efficiency.

2) RELATIONSHIP BETWEEN SHOVEL RESISTANCE AND SHOVEL-PLATE PARAMETERS

Considering the material pushed by the shovel plate, in addition to the compression, fracture, shear resistance of coal and rock and the migration resistance along the shovel surface, the propulsive resistance can be calculated based on the material [44] and ground mechanics [45], as follows:

$$\begin{aligned} F_t = {} & 0.001\eta_c(l_0\delta_0\sigma_n + \mu W_t \cos^2(\beta+\alpha) \\ & + W_t \sin(\beta+\alpha)\cos(\beta+\alpha) \\ & + \frac{lh_c\tau^2}{G} + \frac{l\delta_0\sigma_e^2}{E} + \mu\rho k_c l A_c \cos^2(\beta+\alpha)), \end{aligned} \tag{7}$$

where F_t is the propulsive resistance in kilonewtons (kN), δ_0 is the front-end thickness of the shovel plate in meters (m), l_0 is the cutting length of the front-end of the shovel plate in meters (m), σ_n is the equivalent compressive resistance of the interaction between the shovel plate and extracted material in megapascals (MPa), W_t is the weight of the material on the shovel surface in newtons (N), μ is the friction coefficient between the collected material and shovel surface, h_c is the insertion depth of the shovel loading material in meters (m), τ is the shear stress of the material in megapascals (MPa), G is the shear modulus of the material (mainly coal and rock), E is the bending modulus of the material, k_c is the migration length coefficient of the material, σ_w is the bending stress of the material in megapascals (MPa), ρ is the density of the material in kilograms per cube meter (kg/m^3), α is the inclination angle of the shovel-plate hinge with the ground in degrees (°), A_c is the sectional area of the material in square meters (m^2), and η_c is the mechanical efficiency.

3) CONSTRAINTS ON SHOVEL-PLATE PARAMETERS

According to the shovel-plate working characteristics, structural characteristics, and the actual working conditions shown in Fig. 4, the shovel-plate parameters can be expressed as follows:

$$\begin{cases} L_0 \le l \le L \\ l - 2D - 2l_{xi} > 0 \\ l_z \tan\beta \ge l_q \\ \tan(\beta + \arctan\dfrac{l_x}{l_2}) \le \mu. \end{cases} \tag{8}$$

where L_0 is the lateral width of the track along the displacement direction in meters (m), L is the maximum width for

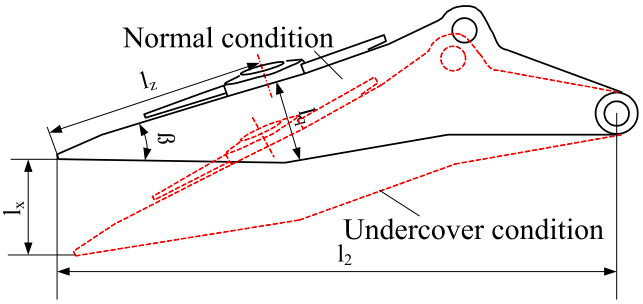

FIGURE 4. Shovel-plate working characteristics.

cutting in meters (m), l_z is the distance between the centerline of the star wheel drive and the front-end of the shovel plate in meters (m), I_q is the thickness of the star wheel drive in meters (m), l_x is the maximum undercover amount of the shovel-plate in meters (m), and l_2 is the length of the shovel-plate in meters (m).

Based on a combination of the ideal point method and the gray weight multiobjective processing method, for increasing the loading capacity and reducing the drag shovel, the resulting multiobjective optimization model can be expressed as follows:

$$\begin{cases} \min f(\mathrm{X}) = \min(W_1 \times \sqrt{(F_t - F_t^*)^2} \\ \qquad + W_2 \times \sqrt{(-Q + Q^*)^2}) \\ L_0 \le l \le L \\ l - 2D - 2l_{xi} > 0 \\ l_z \tan\beta \ge l_q \\ \tan(\beta + \arctan\dfrac{l_x}{l_2}) \le \mu. \end{cases} \tag{9}$$

III. APPLICATION

A. PARAMETER DETERMINATION OF PARTICLE SWARM OPTIMIZATION ALGORITHM

Particle swarm optimization is based on the simulation of the foraging patterns of birds and the determination of the optimal global solution according to the current optimal solution. In PSO, each individual is referred to as a "particle" and represents a potential solution. We assumed a d-dimensional search space with a population of N particles, where $X_i = (x_{i,1}, x_{i,2}, \ldots, x_{i,d})$ and $v_i = (v_{i,1}, v_{i,2}, \ldots, v_{i,d})$ are the d-dimensional position and velocity vector of the $i-th$ particle, respectively. For evaluating the fitness value of each particle, the optimal position $(pbest)\, p_i = (p_{i,1}, p_{i,2}, \ldots, p_{i,d})$ of each particle in the t-th iteration is determined, and the optimal position $(gbest) p_g = (p_{g,1}, p_{g,2}, \ldots, p_{g,d}$ in the group is elucidated. In each iteration, the particle updates its speed and position according to (10):

$$\begin{aligned} v_{i,j}(t+1) = {} & w_k v_{i,j}(t) + c_1 r_1[p_{i,j} - x_{i,j}(t)] \\ & + c_2 r_2[p_{g,j} - x_{i,j}(t)] \\ & \times x_{i,j}(t+1) = x_{i,j}(t) + v_{i,j}(t), j = 1, \ldots, d. \end{aligned} \tag{10}$$

The meaning and value of each parameter in the formula and PSO are based on previous research [28] and are determined as follows: accelerated factor $c_1 = c_2 = 2$, population size N = 20, and iterative algebra S = 100. The maximum speed v_{max} is limited by the range of the parameter values, i.e., $v_{imax} = x_{imax} - x_{imin}$. The inertia factor w is dynamic and decreases linearly, i.e., $w(t) = w_{min} + \frac{w_{max} - w_{min}}{N}$ (N-t). The obtained maximum and minimum inertia factors are $w_{max} = 0.9$ and $w_{min} = 0.4$; r_1 and r_2 are random numbers in the set [0,1]; $p_i = (p_{i,1}, p_{i,2}, \ldots, p_{i,d})$ are the current optimal individual positions of each generation particle, and $p_g = (p_{g,1}, p_{g,2}, \ldots, p_{g,d})$ are the current optimal global positions of each generation population.

Optimization is performed iteratively according to the following process. The population is randomly initialized. Thereafter, the fitness value of each particle is calculated, and *pbest* and *gbest* are determined. Each particle is then adopted according to (7). The fitness values of each particle are recalculated and compared. If the current target value is superior to the previous one, it is used as the updated value. All the current *pbest* and *gbest* are compared, and *gbest* is updated. If the termination condition is satisfied, the algorithm is terminated and the output is optimized; otherwise, the iteration and update are continued.

B. DETERMINATION OF THE IDEAL POINT OF A SINGLE-OBJECTIVE FUNCTION

We considered the EBZ230 roadheader in this study, with basic parameters of $B = 0.62$ m, $D = 1.52$ m, $\eta_m = 0.87$, $\eta_c = 0.85$ and $n = 33$ r/min. Considering that β and l are the most important factors affecting the loading capacity and resistance of the shovel plate and are the most concerned factors of the shovel plate designer, they were selected as design variables. Based on the literature [30], the values of other parameters in Equations (6) to (7) can be determined. Based on the PSO and under the constraints of (8), at $l = 3.14$ m and $\beta = 19.32°$, the ideal loading capacity is $Q^* = 4.19$ m^3/min. Moreover, at $l = 3.1732$ m and $\beta = 14.6°$, the ideal shovel resistance is $F_t^* = 4.14$ kN. The Q^* and F_t^* were obtained through single-objective optimization. The calculation of Q^* and F_t^* are consistent with the optimal solution calculation of the multiobjective function constructed below and are, therefore, not detailed further in this manuscript. The change diagram between the functions (6) and (7) with β and l are shown in Fig. 5.

C. DETERMINATION THE GRAY WEIGHT OF THE SHOVEL RESISTANCE AND LOADING CAPACITY

By visiting several domestic manufacturers of large roadheaders and the associated components, and with reference to relevant information, the parameter values of the shovel-plate series were obtained. The shovel resistance and loading capacity of the roadheader series were calculated according to (6) and (7); these are listed in Table 1.

The shovel resistance and loading capacity data in Table 1 (The EBZ230 parameter is the optimization object and does not participate in this step) were denoted as $\mathbf{A_0}$. Moreover, the shovel resistance was selected as the mother index and the loading capacity was adopted as the subindex. The index value that initializes matrix$\mathbf{A}$ and the correlation coefficient matrix $\mathbf{R}$ can be obtained using (4). The columns of $\mathbf{R}$ can be averaged to obtain $r_1 = 1$ and $r_2 = 0.6371$; the gray weights of the shovel resistance and the loading capacity of the roadheader were obtained as $W_1 = 0.61$ and $W_2 = 0.39$, respectively, via substitution in (5).

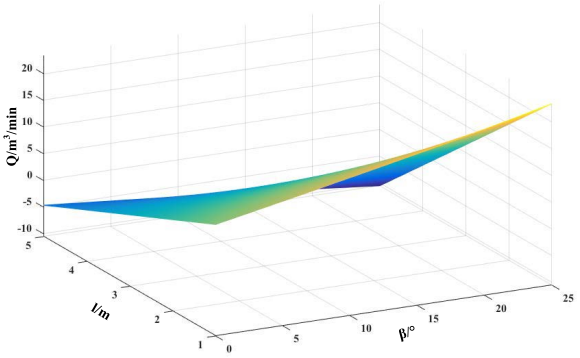

(a) Diagram of relationship between loading capacity with shovel plate parameters

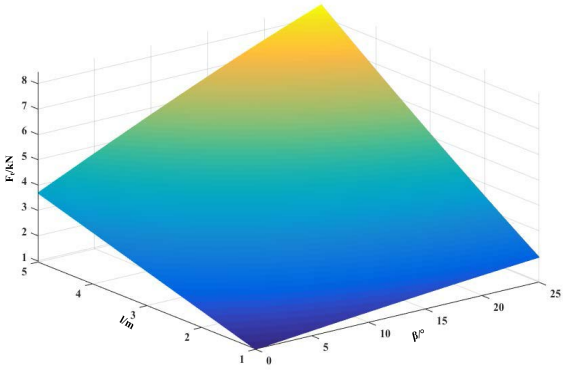

(b) Diagram of relationship between resistance with shovel plate parameters

FIGURE 5. Diagram of relationship between loading capacity and resistance with shovel plate parameters.

TABLE 1. Parameter values of existing shovel plates and calculated shovel resistance and loading capacity.

Roadheader serial number	B (m)	N (r/min)	l (m)	β (°)	F_t (kN)	Q (m^3/min)
EBZ120	0.52	30	2.8	21	4.30	3.10
EBZ135	0.45	33	2.83	22	4.44	3.25
EBZ160	0.54	33	2.9	13.5	3.69	3.38
EBZ200	0.62	33	3.0	20	4.50	3.84
EBZ230(before optimization)	0.62	33	3.2	19	4.67	4.16
EBZ230(After optimization by this paper)	0.62	33	3.15	16.5	4.33	4.22
EBZ260	0.67	35	3.5	18.5	5.03	5.55
EBZ280	0.67	33	3.6	21	5.48	5.93

D. MULTIOBJECTIVE OPTIMIZATION PROCESS AND RESULTS

The corresponding parameter values [30], and $W_1 = 0.61$, $W_2 = 0.39$, $F_t^* = 4.14$ kN, and $Q^* = 4.19$ m^3/min were

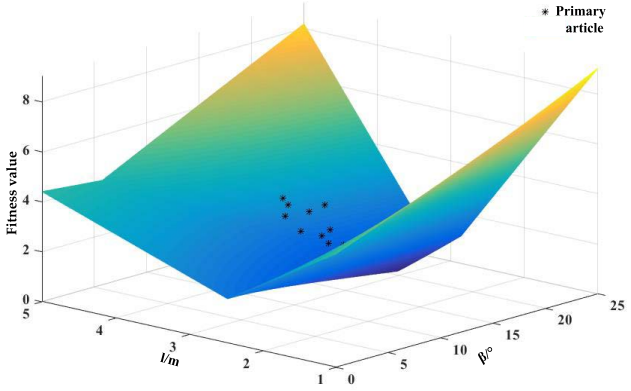

(a) Initial particle distribution position

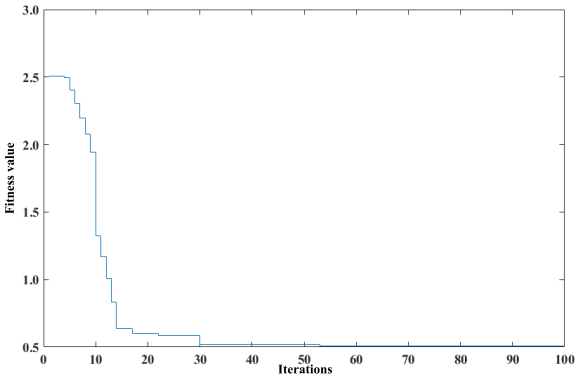

(b) Iterative process

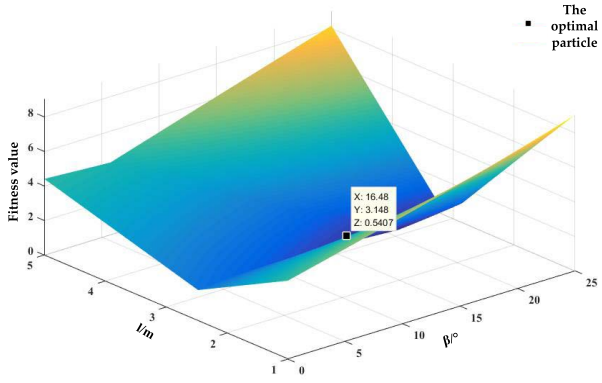

(c) Optimal particle position

FIGURE 6. **Optimization process.**

substituted in the multiobjective function constructed based on (6). The results are expressed by (11):

$$\begin{cases} \min f(\mathrm{X}) = \min(0.61 \times \sqrt{(F_t - 4.14)^2} + 0.39 \\ \times \sqrt{(-Q + 4.19)^2}) \\ 3.14 < l < 6.3 \\ 14.5 < \beta < 19.32. \end{cases} \tag{11}$$

Based on PSO, the particle fitness value and iterative optimization can be realized by considering (11) as the fitness function and restricting the particle activity within the scope of the constraint conditions. PSO algorithm can be applied to constraint optimization problems by limiting the range of particles and adding particle checking mechanism. The particles generated in each iteration are checked by the constraint;

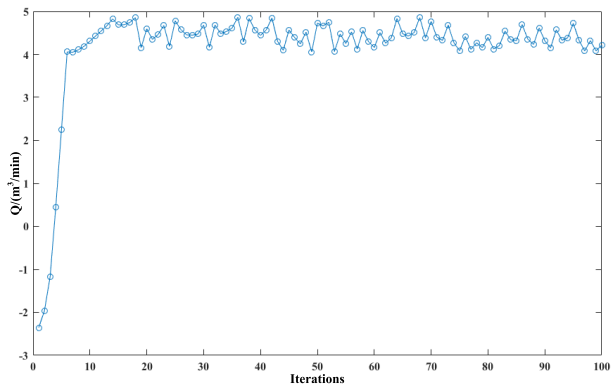

(a) Loading capacity regularity with the optimization process

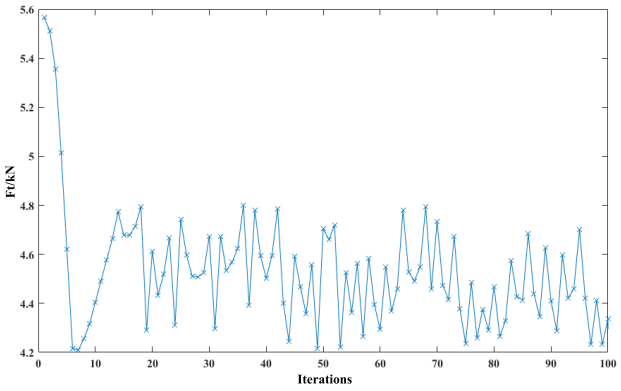

(b) Shovel resistance regularity with the optimization process

FIGURE 7. **Non-inferior solution accumulation regularity with the optimization process.**

the particles out of range are deleted, and the new particles are produced again for inspection. The optimization process is shown in Fig. 6 which shows that the objective function reaches the optimum when the iteration reaches 100 generations. And the non-inferior Q and F_t solution accumulation regularity with the optimization process is shown in Fig. 7 (the optimum particle in each generation of Q and F_t).

Consistent with the optimization objectives, the load capacity converges after gradually increasing, and the propulsive resistance gradually decreases until convergence to a small value. Both Q and F_t are optimized. The non-inferior solution distribution agrees with the overall optimization goal of improving the load capacity and reducing the propulsive resistance. The optimization trends are reasonable, indicating the effectiveness of the PSO algorithm.

IV. RESULTS AND DISCUSSION

A. COMPARISON BEFORE AND AFTER OPTIMIZATION

The obtained optimal particle parameters $l = 3.148$ and $\beta = 16.48°$ were substituted in (6) and (7), and the three-dimensional (3D) model of the shovel plate was established to compare the shovel resistance, loading capacity, and plate quality before and after optimization, as shown in Table 2. To further facilitate comparison, Table 2 lists the optimization results by single ideal point method and single gray weight based on particle swarm optimization algorithm, and the optimization results of genetic algorithm (GA) [46], [47]

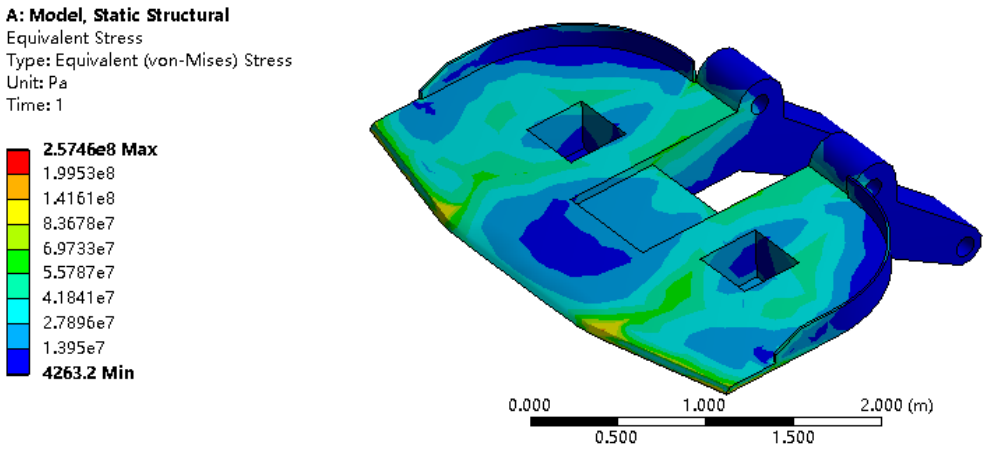

(a) Before optimization

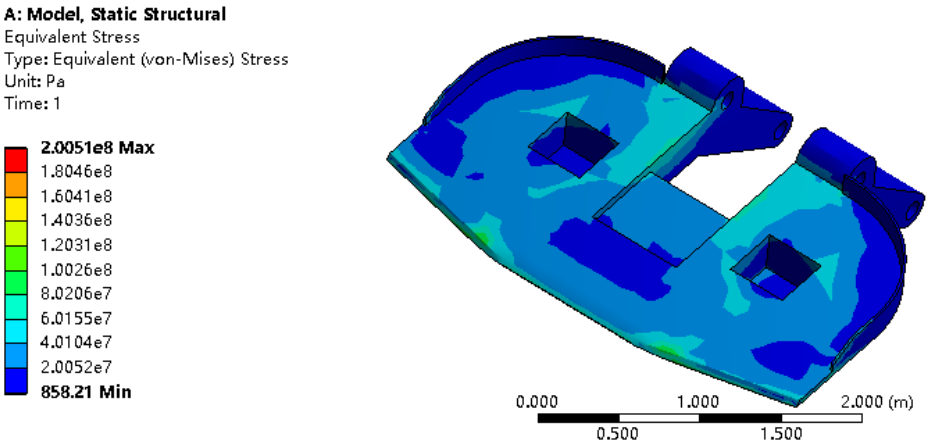

(b) After optimization

FIGURE 8. Roadheader shovel-plate stress nephogram before and after optimization.

TABLE 2. Comparison of EBZ230 Roadheader shovel parameters before and after optimization.

Serial number	Method	l /m	β /°	F_t/N	Q/m^3/min	m/kg
1	Before optimization	3.2	19	4.67	4.16	4597.6
2	Single ideal point by PSO(Q^*)	3.14	19.32	4.62	4.19	-
3	Single ideal point by PSO(F_t^*)	3.17	14.6	4.14	3.51	-
4	Single gray weight by PSO	3.19	17.02	4.46	3.99	-
5	Combined the ideal point and gray weight by Genetic Algorithm	3.148	16.32	4.30	4.21	-
6	Combined the ideal point and gray weight(The method recommended in this article)	3.15	16.5	4.33	4.22	3942.2
7	Optimization improvement(Compare row 1 and row 6)	1.5%	13.2%	7.3%	1.4%	14.3%

based on the combination of ideal point method and gray weight. The optimization process is similar to the one detailed above.

Table 2 shows that the ideal point method and gray weight method for constructing an objective function for multiobjective optimization can achieve better optimization results and every goal has been optimized. The ideal-point method is just a single goal to achieve the optimum. The single gray weight ensures optimization of every goal, although with a low degree of optimization. The combination of ideal point method and gray weight based on PSO and GA achieve similar optimization results, while the PSO is a slightly better.

With a change in the shovel parameters after optimization, the mass of the shovel plate decreases by 14.3%, the

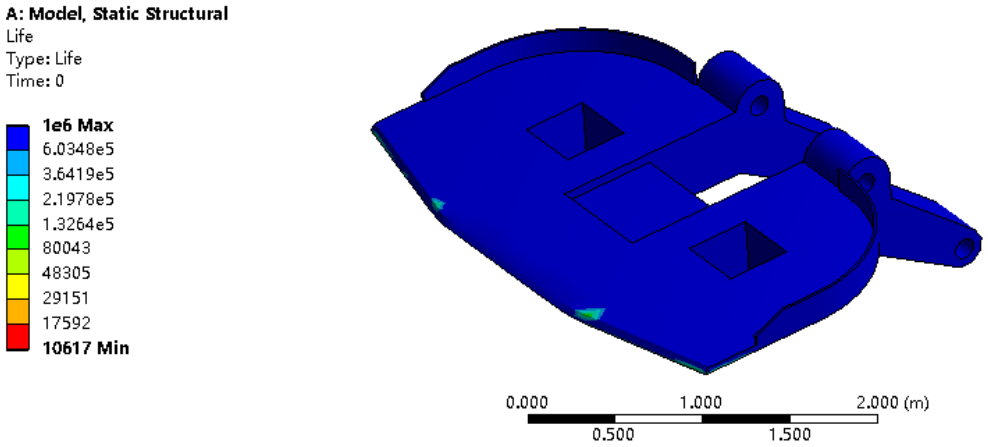

(a) Before optimization

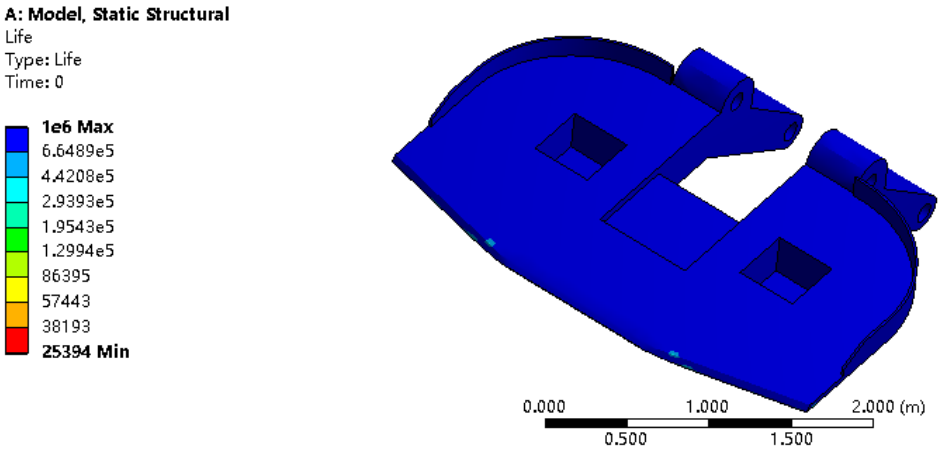

(b) After optimization

FIGURE 9. Roadheader shovel-plate fatigue life nephogram before and after optimization.

TABLE 3. Key mechanical properties of Q345.

Density (kg/m^3)	Yield strength (MPa)	Elasticity modulus (GPa)	Tensile strength (MPa)	Poisson's ratio
7850	345	200	470~650	0.2

propulsive resistance decreases by 7.3%, and the load capacity increases by 1.4%.

To analyze the mechanical properties of the shovel plate in the ANSYS-Workbench environment, propulsive coal rock with the shovel plate before and after optimization was simulated at the maximum propulsive resistance. The actual material used for the shovel plate is Q345. And the key mechanical properties of the Q345 is given in table 3.

The mean-stress theory used in the ANSYS fatigue tool is Goodman theory. The stress, fatigue life, and safety factor nephograms of the shovel-plate before and after optimization are shown in Figs. 8–10, respectively.

Fig. 8 displays the stress nephogram before and after optimization. Before and after optimization, the position of the maximum stress area did not change, which was in the middle position of the front section of the shovel plate. After optimization, the area with large force is larger than that before optimization, which means that the stress is more uniform. After optimization, some forces are evenly loaded to the rear of the shovel plate (the wathet blue part in the FIG. 8), which shows that the bearing design of the shovel plate is more reasonable. The maximum stress at the front of the shovel plate before and after optimization is 257.5 MPa and 200.5 MPa, respectively, which corresponds to a decrease of 22.1%.

Fig. 9 presents the fatigue life nephogram before and after optimization. The fatigue life danger area after optimization is smaller than that before optimization (colored area in Fig. 9). The minimum fatigue life of the shovel plate before and after optimization is 1.06×10^4 and 2.54×10^4, respectively, which corresponds to an increase of 139.6%.

Fig. 10 depicts the safety factor nephogram before and after optimization. After optimization, the safety area of the shovel plate becomes more uniform than that before optimization (green and yellow parts in Fig. 10), which also shows that the load bearing design of the shovel plate is more reasonable. The minimum safety factor of the shovel plate before and after optimization is 0.33 and 0.43, respectively, which corresponds to an increase of 30.3%.

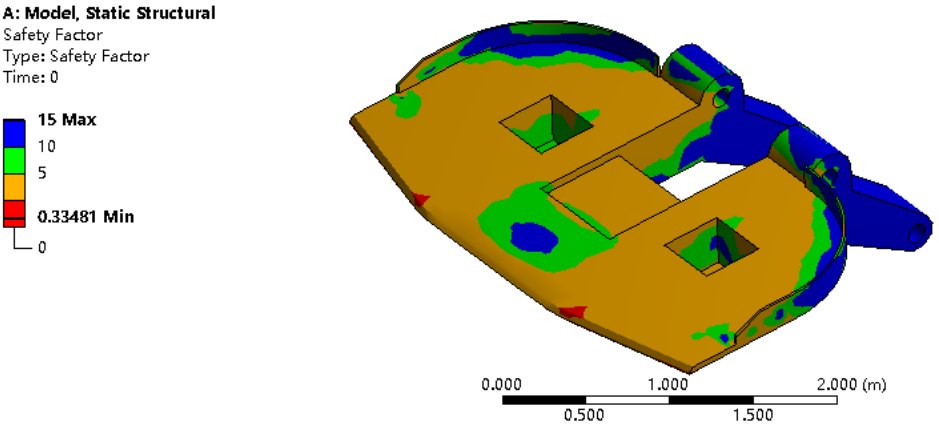

(a) Before optimization

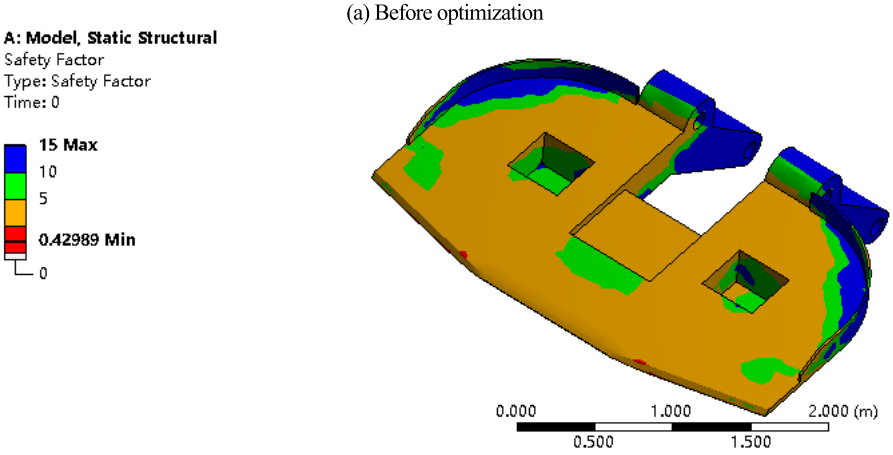

(b) After optimization

FIGURE 10. Roadheader shovel-plate safety factor nephogram before and after optimization.

After optimization, the loading capacity improves, the shovel resistance and mass reduce, and the mechanical properties are enhanced. These results indicate improvement in the EBZ230 roadheader shovel plate, previously mass-produced without optimization. The abovementioned findings demonstrate the potential for enhancement through optimization of previously manufactured roadheader shovels.

B. APPLICATION PROSPECTS

As previously mentioned, multiobjective optimization is a critical aspect of scientific research and engineering practice [48]. On the one hand, traditional methods for solving multiobjective problems including the constraint method, weighted combination method, and goal programming method require considerable prior knowledge and experience. In addition, they are only effective for specific problems, and cannot yield satisfactory results [49]. On the other hand, in engineering practice, each objective function has a different physical meaning and dimensionality, and the degree of consideration is not consistent; thus, the importance of each objective function cannot be distinguished based on the ideal point method [50]. Moreover, the simple linear weighting method is excessively subjective, complex, expensive, and difficult to implement, as experts and professionals in the field are required to determine the weights [51].

This study developed a method combining the ideal point method and gray weight method for constructing an objective function for multiobjective optimization.

The advantages of the proposed method as follows: 1) The importance of each objective function is considered, and the weight of each objective function can be determined without the need for organizational domain experts, which can reduce organizational costs and realize multiobjective optimization more rapidly and conveniently. 2) It can also overcome the problem of the ideal point method not being able to reflect the importance of each objective function.

The limitations of the proposed method are as follows: 1) The data on existing series of products is required for determination of gray weight. 2) Gray weights need to be calculated by the method and process described in this paper, which is not yet integrated with the optimization algorithm.

The proposed method was successfully applied for the multiobjective optimization of the shovel-plate parameters of a roadheader, and a significant degree of optimization was realized. The method and application process can be extended to the multiobjective optimization design of other devices as well. The proposed method is applicable to other types of machines and is particularly suitable for multiobjective structure optimization.

V. CONCLUSION

To optimize the roadheader shovel-plate parameters, we proposed the ideal point method and gray weighting for multiobjective optimization. We performed simulation analyses and compared the excavation of coal rock with a shovel plate before and after optimization. The study can be summarized as follows:

1) This study developed a method combining the ideal point method and gray weight method for constructing an objective function for multiobjective optimization. Moreover, a method for objectively determining the index weight coefficient is provided.

2) The gray weights of the loading capacity and shovel resistance were determined as $W_1 = 0.6108$ and $W_2 = 0.3892$, respectively, by investigating the existing molded products and objectively determining the index weight coefficient.

3) A mathematical model of the loading capacity and shovel grubbing force with the shovel-plate parameters was established. Particle swarm optimization was used to optimize the multiobjective parameters of the shovel plate. Considering the EBZ230-type roadheader shovel plate as an example, the optimized scraper parameters through multiobjective optimization decreased the mass of the shovel plate by 14.3% and shovel resistance by 7.3%, while increasing the loading capacity by 1.4%.

4) Coal and rock excavation before and after shovel-plate optimization was simulated in an ANSYS-Workbench environment. The simulation results indicated that the maximum stress at the front of the shovel plate was 257.5 MPa and 200.2 MPa before and after optimization, respectively, corresponding to a decrease of 22.1%. The minimum fatigue life was 1.06×10^4 and 2.54×10^4 before and after optimization, respectively, corresponding to an increase of 139.6%. Moreover, the minimum safety factor was 0.33 and 0.43 before and after optimization, respectively, corresponding to an increase of 30.3%.

The abovementioned results demonstrate that the method combining the ideal point method and gray weight method for constructing an objective function for multiobjective optimization and with PSO optimizes the shovel-plate parameters. The findings of this study can provide a specific theoretical basis and reference values for the design of roadheader shovel plates and can serve as a reference for multiobjective optimization problems in engineering.In this study, the multiobjective optimization of roadheader shovel plate was verified theoretically and through simulations. And we hope that this method can be applied to more optimization design of roadheader parts. We are working on other applications such as cutting head optimization for shield machines. The proposed method is applicable to other types of machines and is particularly suitable for multiobjective structure optimization.

However, to compare the theoretical and experimental results remains to be addressed. Moreover, the sensitivity of weight coefficient has not been analyzed. In future, we plan to continue our experimental and theoretical comparative studies, including sensitivity analysis of weight coefficient.

ACKNOWLEDGMENT

The authors are very grateful to the editors and reviewers.

REFERENCES

[1] *Outline of the National Program for Medium- and Long-term Scientific and Technological Development (2006–2020)*, Bulletin of The State Council of the People's Republic of China, Beijing, China, 2006, pp. 1–5, vol. 9.

[2] Y. A. Wu, J. Wu, G. De, and W. Fan, "Research on optimal operation model of virtual electric power plant considering net-zero carbon emission," *Sustainability*, vol. 14, no. 6, pp. 16–20, 2022.

[3] *Information Office of the State Council of the People's Republic of China Fan*, China's Energy Policy, Hangzhou, China, 2012, vol. 10.

[4] O. Acaroglu and C. Erdogan, "Stability analysis of roadheaders with mini-disc," *Tunnelling Underground Space Technol.*, vol. 68, pp. 187–195, Sep. 2017.

[5] (Jul. 31, 2020). *Sina Finance. Guideline on High Quality Development of Coal Industry during the 14th Five-Year Plan Period (Draft)*. [Online]. Available: https://baijiahao.baidu.com/s?id=1673718418080060393&wfr=spider&for=pc

[6] (Dec. 14, 2021). *The Coal Business: Guiding Opinions on the Construction of Safe and Efficient Coal Mines in the 14th Five-Year Plan for Coal Industry*. [Online]. Available: https://view.inews.qq.com/a/20211214A0BVII00

[7] H.-E. Nam, K.-M. Kyeon, T.-S. Rehman, H. Yoo, and H.-K., "Analysis of the effect of the tool shape on the performance of pre-cutting machines during tunneling using linear cutting tests," *Appl. Sci.*, vol. 12, no. 4489, pp. 1–18, Apr. 2022.

[8] C. Z. Zhang, H. Huang, and G. D. Yang, "Design of roadheader shovel board," *Coal Mine Machin.*, vol. 34, no. 7, pp. 5–6, 2013.

[9] H. Wang, D. Sun, and D. A. Qin, "New continuously variable transmission system applied to transmission system of the roadheader's cutting unit," *Proc. Inst. Mech. Eng., C, J. Mech. Eng. Sci.*, vol. 231, no. 9, pp. 3590–3600, 2016.

[10] M. Zhang, F. Lyu, X. Tang, Y. Yang, X. Ji, and M. Wu, "Analysis of vibration of roadheader rotary table based on finite element method and data from underground coalmine," *Shock Vibrat.*, vol. 2018, pp. 1–10, Jan. 2018.

[11] M. Zhang, F. Lyu, C. Li, X. Li, and M. Wu, "The roadheader auto-rectification dynamic analysis and control based on the roadway floor mechanic characteristics," *Arabian J. Sci. Eng.*, vol. 46, no. 3, pp. 2649–2661, Mar. 2021.

[12] Y. Shen, P. Wang, W. Zheng, X. Ji, H. Jiang, and M. Wu, "Error compensation of strapdown inertial navigation system for the boom-type roadheader under complex vibration," *Axioms*, vol. 10, no. 3, p. 224, Sep. 2021.

[13] X. Ji, M. Zhang, Y. Qu, H. Jiang, and M. Wu, "Travel dynamics analysis and intelligent path rectification planning of a roadheader on a roadway," *Energies*, vol. 14, no. 21, p. 7201, Nov. 2021.

[14] C. Liu, M. Gao, G. Zhu, C. Zhang, P. Zhang, J. Chen, and W. Cai, "Data driven eco-efficiency evaluation and optimization in industrial production," *Energy*, vol. 224, pp. 1–11, Feb. 2021.

[15] L. Fang, Z. Liu, and M. Wu, "Intelligent optimal control considering dynamic posture compensation for a cantilever roadheader," *Robotica*, vol. 40, no. 3, pp. 583–598, Mar. 2022.

[16] C. Z. Zhang, H. Huang, and G. D. Yang, "Design of roadheader shovel board," *Coal Mine Mach.*, vol. 34, pp. 5–6, Jan. 2013.

[17] C. Liu, J. Chen, and W. Cai, "Data-driven remanufacturability evaluation method of waste parts," *IEEE Trans. Ind. Informat.*, vol. 18, no. 7, pp. 4587–4595, Jul. 2022.

[18] Z. Nie, S. Jung, L. B. Kara, and K. S. Whitefoot, "Optimization of part consolidation for minimum production costs and time using additive manufacturing," *J. Mech. Des.*, vol. 142, no. 7, Jul. 2020, Art. no. 072001.

[19] P. Moore and G. K. Venayagamoorthy, "Evolving combinational logic circuits using a hybrid quantum evolution and particle swarm inspired algorithm," in *Proc. NASA/DoD Conf. Evolvable Hardw. (EH)*, Jun. 2005, pp. 97–102.

[20] S. M. Mikki and A. A. Kishk, "Quantum particle swarm optimization for electromagnetics," *IEEE Trans. Antennas Propag.*, vol. 54, no. 10, pp. 2764–2775, Oct. 2006.

[21] Z. Zhang, Q. Yu, J. Hu, and X. Zhu, "Hybrid particle swarm optimization algorithm for balancing problem of stochastic mixed-model assembly line," *Mach. Des. Res.*, vol. 29, no. 2, pp. 60–63, 2013.
[22] L. Wei, L. Wang, M. Ma, H. Che, and J. Yang, "Optimization of tandem cold rolling schedule based on improved multi- objective particle swarm optimization algorithm," *China Mech. Eng.*, vol. 36, pp. 1239–1242, Jan. 2015.
[23] Q. Hou, M. Wang, and X. Zhou, "Improved DEA cross efficiency evaluation method based on ideal and anti-ideal points," *Discrete Dyn. Nature Soc.*, vol. 2018, pp. 1–9, Apr. 2018.
[24] G. Dinde and G. S. Dhende, "Study of machining parameters for wet turning of F55 stainless steel using grey relational analysis for improvement in surface roughness," in *Optimization Methods in Engineering* (Lecture Notes on Multidisciplinary Industrial Engineering), M. Tyagi, A. Sachdeva, and V. Sharma, Eds. Singapore: Springer, 2021, pp. 567–578.
[25] J. Sun, W. Chen, W. Fang, X. Wun, and W. Xu, "Gene expression data analysis with the clustering method based on an improved quantum-behaved particle swarm optimization," *Eng. Appl. Artif. Intell.*, vol. 25, no. 2, pp. 376–391, Mar. 2012.
[26] S. Mirjalili and J. Dong, *Multiobjective Optimization Using Artificial Intelligence Techniques*. Cham, Switzerland: Springer, 2020, pp. 10–12.
[27] W. Xu, M. M. Ismail, Y. Liu, and M. Islam, "Parameter optimization of adaptive flux-weakening strategy for permanent-magnetsynchronous motor drives based on particle swarm algorithm," *IEEE Trans. Power Electron.*, vol. 34, no. 12, pp. 12128–12140, Dec. 2019.
[28] Y. Marinakis, M. Marinaki, and G. Dounias, "A hybrid particle swarm optimization algorithm for the vehicle routing problem," *Eng. Appl. Artif. Intell.*, vol. 23, no. 4, pp. 463–472, 2010.
[29] X. Xia, Y. Xing, B. Wei, Y. Zhang, X. Li, X. Deng, and L. Gui, "A fitness-based multi-role particle swarm optimization," *Swarm Evol. Comput.*, vol. 44, pp. 349–364, Feb. 2019.
[30] G. Xu, Q. Cui, and X. Shi, "Particle swarm optimization based on dimensional learning strategy," *Swarm Evol. Comput.*, vol. 45, pp. 33–51, Mar. 2019.
[31] S. Mirjalili, "A sine cosine algorithm for solving optimization problems," *Knowl.-Based Syst.*, vol. 96, pp. 120–133, Mar. 2016.
[32] S. Mirjalili, S. M. Mirjalili, and A. Hatamlou, "Multi-verse optimizer: A nature-inspired algorithm for global optimization," *Neural Comput. Appl.*, vol. 27, no. 2, pp. 495–513, Feb. 2016.
[33] X.-S. Yang, "Firefly algorithm stochastic test functions and design optimisation," *Int. J. Bio-Inspired Comput.*, vol. 2, no. 2, pp. 78–84, 2010.
[34] W. Gao, L. Hu, Y. Li, and P. Zhang, "Preserving similarity and staring decisis for feature selection," *IEEE Trans. Artif. Intell.*, vol. 2, no. 6, pp. 584–593, Dec. 2021.
[35] S. Zhao, M. Wang, S. Ma, and Q. Cui, "A feature selection method via relevant-redundant weight," *Expert Syst. Appl.*, vol. 207, Nov. 2022, Art. no. 117923, doi: 10.1016/j.eswa.2022.117923.
[36] H. Alazzam, A. Sharieh, and K. E. Sabri, "A feature selection algorithm for intrusion detection system based on pigeon inspired optimizer," *Expert Syst. Appl.*, vol. 148, Jun. 2020, Art. no. 113249, doi: 10.1016/j.eswa.2020.113249.
[37] A. Kaveh and S. Talatahari, "Size optimization of space trusses using big bang–big crunch algorithm," *Comput. Struct.*, vol. 87, nos. 17–18, pp. 1129–1140, Sep. 2009. [Online]. Available: http://www.sciencedirect.com/science/article/pii/S0045794909001394
[38] I. Ahmadianfar, A. A. Heidari, A. H. Gandomi, X. Chu, and H. Chen, "RUN beyond the metaphor: An efficient optimization algorithm based on Runge Kutta method," *Expert Syst. Appl.*, vol. 181, Nov. 2021, Art. no. 115079.
[39] C. Blum and A. Roli, "Metaheuristics in combinatorial optimization: Overview and conceptual comparison," *ACM Comput. Surv.*, vol. 35, no. 3, pp. 268–308, 2003.
[40] Z. He, J. Zhou, L. Mo, H. Qin, X. Xiao, B. Jia, and C. Wang, "Multi-objective reservoir operation optimization using improved multiobjective dynamic programming based on reference lines," *IEEE Access*, vol. 7, pp. 103473–103484, 2019.
[41] G. Dhiman and V. Kumar, "Spotted hyena optimizer: A novel bio-inspired based metaheuristic technique for engineering applications," *Adv. Eng. Softw.*, vol. 114, pp. 48–70, Dec. 2017.
[42] G. Dhiman and V. Kumar, "Seagull optimization algorithm: Theory and its applications for large-scale industrial engineering problems," *Knowl.-Based Syst.*, vol. 165, pp. 169–196, Nov. 2019.
[43] S. Zhao, T. Zhang, S. Ma, and M. Chen, "Dandelion Optimizer: A nature-inspired metaheuristic algorithm for engineering applications," *Eng. Appl. Artif. Intell.*, vol. 114, pp. 1–20, Sep. 2022.
[44] J. Li, J. He, Y. Xing, and F. Gao, "Dimensional optimization of rocker-bogie suspension for planetary rover based on kinetostatics and terramechanics," *Proc. Inst. Mech. Eng., C, J. Mech. Eng. Sci.*, vol. 236, no. 1, pp. 246–262, Jan. 2022.
[45] T. L. Li, X. M. Wu, and H. Z. Tu, "The measurement and analysis and application on the mechanical property of coal seam," *Geol. Prospecting*, vol. 36, no. 2, pp. 85–88, 2000.
[46] H. Fourati, R. Maaloul, L. Fourati, and M. Jmaiel, "An efficient energy-saving scheme using genetic algorithm for 5G heterogeneous networks," *IEEE Syst. J.*, no. 1, pp. 1–12, Apr. 2022, doi: 10.1109/JSYST.2022.3166228.
[47] Y. Yu, J. Mo, Q. Deng, C. Zhou, B. Li, X. Wang, N. Yang, Q. Tang, and X. Feng, "Memristor parallel computing for a matrixfriendly genetic algorithm," *IEEE Trans. Evol. Comput.*, early access, Jan. 21, 2022, doi: 10.1109/TEVC.2022.3144419.
[48] G. V. Chakaravarthy, S. Marimuthu, and A. N. Sait, "Performance evaluation of proposed differential evolution and particle swarm optimization algorithms for scheduling m-machine flow shops with lot streaming," *J. Intell. Manuf.*, vol. 24, no. 1, pp. 175–191, Feb. 2013.
[49] J. Sun, W. Chen, W. Fang, X. Wun, and W. Xu, "Gene expression data analysis with the clustering method based on an improved quantum-behaved particle swarm optimization," *Eng. Appl. Artif. Intell.*, vol. 25, no. 2, pp. 376–391, Mar. 2012.
[50] S. M. Mikki and A. A. Kishk, "Quantum particle swarm optimization for electromagnetics," *IEEE Trans. Antennas Propag.*, vol. 54, no. 10, pp. 2764–2775, Oct. 2006.
[51] M. S. Leu and M. F. Yeh, "Gray particle swarm optimization," *Appl. Soft. Comput.*, vol. 12, pp. 2985–2996, Jan. 2012.

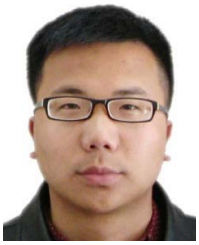

QIANG LI was born in Yingshan, Hubei, China, in 1987. He is currently pursuing the Ph.D. degree with the China University of Mining and Technology. He is also a Lecturer at Suzhou University. His main research interests include rapid tunneling technology of tunnels and roadways, and multiobjective optimization.

SONGYONG LIU was born in Shijiazhuang, Hebei, China, in 1981. He received the Ph.D. degree in mechanical design and theory from the China University of Mining and Technology, Xuzhou, China, in 2009. Since 2015, he has been a Professor at the School of Mechatronic Engineering, China University of Mining and Technology. He has authored two books, more than 50 articles, and more than 76 inventions. His research interests include the design and dynamics of excavation machinery, and automatic systems.

MENGDI GAO was born in 1991. She received the Ph.D. degree in mechanical and electronic engineering from the Hefei University of Technology, Hefei, China, in 2017. She is currently the Head of the 3D Printing Laboratory, Suzhou University. She has published more than 20 academic articles, including the *Journal of Dynamic Systems, Measurement, and Control* (ASME), *IJAMT*, and *Energy Conversion and Management*. Her current research interests include green design and manufacturing, 3D printing technology, manufacturing process condition monitoring, low-carbon energy-saving optimization theory, and multi-objective optimization and methods. She has been invited to be a reviewer for several SCI/EI journals.